Evaluation of a Twin-Spool Hydrogen Turbopump at Zero NPSP

E. K. Bair* and W. E. Campbell†
Aerojet-General Corporation, Sacramento, Calif.

Results of a test program to confirm the prediction of performance and operational characteristics of a prototype twin-spool (integrated low-speed inducer, high-speed pump) hydrogen turbopump at zero net positive suction pressure (NPSP: saturated fluid in the propellant tank) are described. Steady-state and simulated engine transient performance at NPSP values from 20 psi to 0 psi, with hydrogen temperatures of 37°R to 38°R, and with substantial vapor ingestion, are summarized over the operating range of the pump. This member of the low-speed inducer-equipped turbopump family incorporates an inducer forward of the main pump which is driven through a coaxial shaft by a single-stage gas turbine located aft of the main turbine. In previous hydrogen testing, the positive NPSP main turbopump exhibited inadequate pressure rise and flow range at zero NPSP. Testing with the low-speed stage provided a direct evaluation of its addition upon over-all turbopump performance and behavior.

Introduction

NET positive suction pressure (NPSP) is defined herein as the margin of propellant total pressure above vapor (saturation) pressure and is measured in the propellant tank. Zero NPSP is that condition where the tank absolute pressure and the propellant saturation pressure are the same. The term NPSH simply is the conversion of the NPSP pressure term into head (ft), using the appropriate density.

Strong evidence exists that operation at zero NPSP can provide increased performance and reliability. Conditions from which both chemical and nuclear engine systems can benefit are reduced tank weight, possible elimination of the pressurization system, reduced tank interior complexity, and easier stage/engine integration. Increased reliability results from extended operating margins and reduced tank/engine interactions. In a nuclear rocket, the increase in performance results from the ability to pump otherwise unusable tank residuals along with a reduction in the nuclear shielding required.

Recognizing the value of a zero NPSP propellant feed system, the NASA Lewis Research Center instituted a series of technology investigations to explore and compare various low-speed inducer concepts for turbopumps. These included the full-flow and part-flow hydraulic turbine driven inducers as well as the hubless inducer approach.

Independent of these concepts, Aerojet-General Corporation (AGC) proceeded with a company sponsored effort to design and fabricate a twin-spool turbopump for zero NPSP operation in liquid hydrogen. As a companion concept to the other NASA programs, a contract was awarded to AGC for the testing of this turbopump. This paper presents the results of that program.

Technical Discussion

The twin-spool turbopump (Figs. 1 and 2) is a modification of an existing single-shaft turbopump, with a centrifugal pump driven by a two-stage impulse turbine. The basic turbopump was modified to add an in-line, low-speed inducer in front of the main pump inlet and an inducer drive turbine just behind the main turbine which extracts its power from the main turbine exhaust gas. The inducer and turbine are mechanically-connected by a shaft that is coaxial with the hollow main turbopump shaft. Both the inducer and main stages are supported by their own liquid-hydrogen-cooled rolling element bearings.

The main turbopump selected for conversion to a twin-spool configuration had been used in previous liquid hydrogen (LH_2), zero NPSP experiments conducted during October 1966.[1] In these tests, the NPSP had a very significant effect on over-all performance, as shown in Fig. 3. The selected configuration provided the unique opportunity to determine the effects of adding the inducer stage to the main turbopump. In addition, the basic concept was expected to provide excellent stage-transient response because the power is applied to both stages almost simultaneously since the inducer turbine is located close to the main turbine exit.

Although AGC had conducted zero NPSP pumping tests at inlet velocities of 40 fps, and tip speeds from 400 fps to 500 fps, a more conservative criteria were used in designing the inducer.[1–5] The inducer design criteria used for this machine are presented in Table 1 and reflect demonstrated values, while accounting for the advantage to be derived from only 80 ft (a conservative value) of thermo-

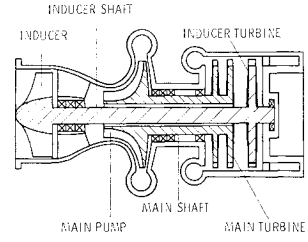

Fig. 1 Twin-spool turbopump schematic.

Presented as Paper 69-550 at the AIAA 5th Propulsion Joint Specialist Conference, U.S. Air Force Academy, Colo., June 9–13, 1969; submitted July 10, 1969; revision received September 26, 1969. The authors thank the Space Nuclear Propulsion Office of NASA for their cooperation, permission for use of the main turbopump, and testing facility, and provision of the necessary propellants. In addition, they acknowledge the efforts of the following Aerojet, Nuclear Rocket Operations personnel in conducting this program: F. X. Andrews for project test operations and K. G. Kirk for computer analysis and development.

* Supervisor, Turbomachinery Special Projects, Nuclear Rocket Operations. Member AIAA.

† Manager, Turbomachinery, Nuclear Rocket Operations. Member AIAA.

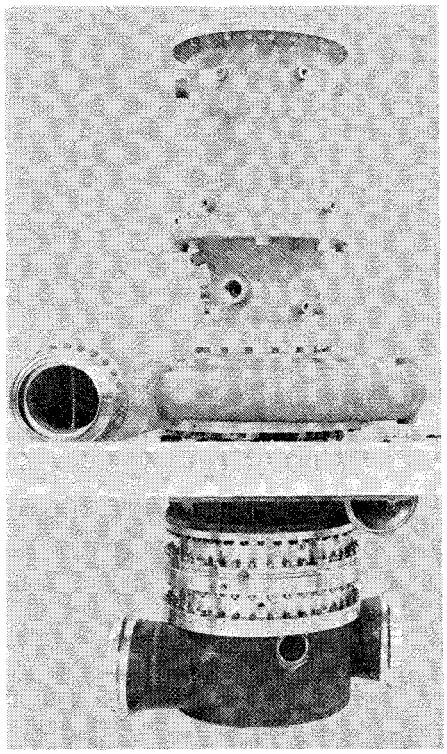

Fig. 2 Turbopump assay—twin spool.

dynamic suppression head (TSH), or thermodynamic effect upon cavitation (TEC).

The flow range selected for investigation was from 45 lb/sec to 77 lb/sec because it provided a comparison with other low-speed inducer concepts under study and matched the data taken from the initial zero NPSP tests.

The unit was modeled analytically using a digital computer. Predicted operating maps were generated. The nominal ratio of inducer horsepower to main-pump horsepower was found to be 0.049. The prediction indicated that, 1) the twin-spool turbopump performance would be insensitive to variation in tank pressure for a wide range of flow rates, 2) the stall margin of the pump would not be reduced when operating at low-suction pressures, and 3) the engine could be hydrodynamically decoupled from the tank by the twin-spool system, which makes pressure rise (and engine thrust) less sensitive to tank conditions.

The specific objectives of the program were 1) develop a digital computer program to predict the steady-state and transient performance of the twin-spool turbopump, both cavitating and noncavitating, 2) establish the operational characteristics of the twin-spool turbopump and experimentally verify the computer prediction method as well as to provide appropriate refinements to the mathematical computerized model based upon the experimental results, 3) establish a basis for making a turbopump configuration

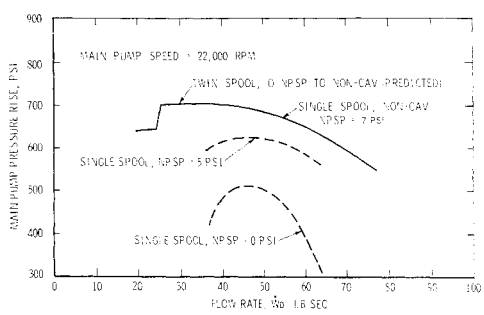

Fig. 3 Performance comparison—single- and twin-spool turbopumps.

Table 1 Inducer design criteria for zero NPSP operation

Maximum inducer inlet axial velocity	40 fps
Maximum inducer inlet tip speed	500 fps
Maximum $N \times Q^{1/2}$	1×10^6 (rpm) $\times$ (gpm)$^{1/2}$
Minimum inducer inlet temperature	36.5°R
Maximum available thermodynamic suppression head	80 ft

selection (single-spool or twin-spool) for engine applications, 4) provide comparison data for this inducer-drive system that is comparable to that acquired with other low-speed inducer concepts, and 5) provide engine system integration design data in the form of transient and steady-state performance.

Computer Model

The computer program generated for simulation of the twin-spool turbopump is divided into subroutines, each of which can be evaluated as a separate entity. Characteristic turbopump component parametric data serve as the primary input to the system. The model logic can be used for either steady-state or transient predictions. The program can be refined using actual characteristics established by testing as the input. It can handle any desired propellant, and the design may be changed simply by substituting new pump and turbine characteristic curves and the inducer and main rotor polar moments of inertia.

The predicted main pump operating map is shown in Fig. 4. This map, which is independent of NPSP, is based upon the nominal turbine exhaust configuration (i.e., no orifice). Predicted inducer speed lines are superimposed.

A predicted 3-sec start transient is shown in Fig. 5, with appropriate inducer and main turbopump parameters plotted against time. Transient predictions are based upon finite time difference calculations and consider the inertia effect of both stages. The options available for defining the ramp profile include shaft speed, turbine-inlet pressure, and turbine-inlet temperature. Any desired profile is possible, because the input is in tabular form. This feature is especially useful when comparing predicted data with actual data. The program includes the dynamic effects of the pump inlet and discharge lines.

Test Program

The test program was designed to investigate pertinent operating characteristics as they would relate to both chemical and nuclear propulsion systems. The following were included in the test plan: 1) flow mapping at half-speed

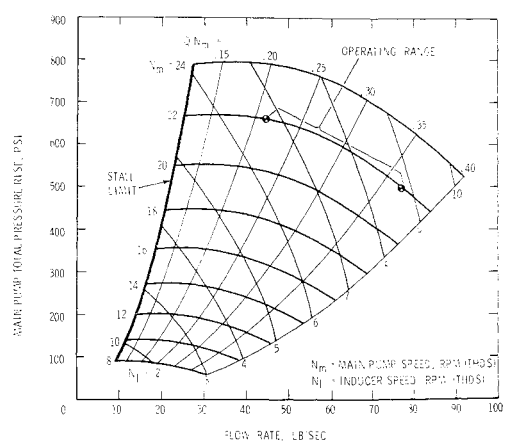

Fig. 4 Predicted operating map.

and full-speed with NPSP values of 20, 5, and 0 psi, 2) NPSP traverses ranging from 20 psi to 0 psi at full-speed with selected constant flow rates, 3) two 3-sec start ramps with terminal NPSP's of 20 psi and 1 psi and a 6-sec start ramp with NPSP reaching 0 psi at the end, and 4) two tests of inducer stage sensitivity to variations in exhaust line area were conducted. The pressure ratio division between the main turbine and the inducer turbine was varied by placing restricting orifices in the turbine exhaust line.

Figure 6 is a graphic outline of the test program. Testing was conducted in the H-6 turbopump test facility at AGC. The run tank has a capacity of 60,000 lb of LH_2 (110,000 gal). A transfer line extends from the bottom of the run tank to a simulated tank bottom, where the LH_2 passes through straightening vanes and is diffused into a 24-in.-diam section. The fluid then is accelerated slightly through a bellmouth transition section as it enters the turbopump inlet line (Fig. 7).

Pump discharge flow is transferred to a 110,000-gal capacity spherical catch vessel. Hydrogen gas is flared-off through the vent stack above the catch vessel. Gaseous hydrogen at ambient temperature (from a high-pressure cascade or bottle farm) is used to drive the turbine.

The 112 turbopump data measurements taken during each test included pressures, temperatures, flow rate, shaft speed, vibration, and selected high-frequency pressures. Data acquisition equipment consisted of strip charts, magnetic tapes, oscillographs, and analog-to-digital converters (ADC). Continuous ADC recordings were taken in all tests. Turbopump operation was initiated after the unit had been chilled to thermal equilibrium.

During tests where data points were taken at a constant speed, the start ramps were made with a constant pump discharge valve setting. After the main-stage shaft speed was achieved, Q/N and N (speed) controls were activated. These control systems regulated the pump discharge and turbine power control valve positions and allowed rapid data point transfer at a fixed speed by a simple Q/N setting change.

The transient start-ramp controls applied turbine power in a programmed form. A fixed-pump discharge valve setting was maintained for the initial portion of the ramp, then the Q/N controller completed the ramp to full speed. When sampling steady-state data, the NPSP was regulated by monitoring the fluid pressure and temperature at two stations: 53 in. above the pump inlet, in the 24-in. simulated tank bottom, and in the 10-in.-diam inlet line 26-in. upstream of the pump inlet. For positive values of NPSP, the run vessel ullage pressure was regulated until the desired margin of pump inlet pressure above saturation pressure was achieved. For zero NPSP operation, the ullage pressure was lowered until saturation pressure was achieved at stations 53 and 26. From this point, the pressure was further reduced until a temperature shift occurred at station 26 (10-in. diam).

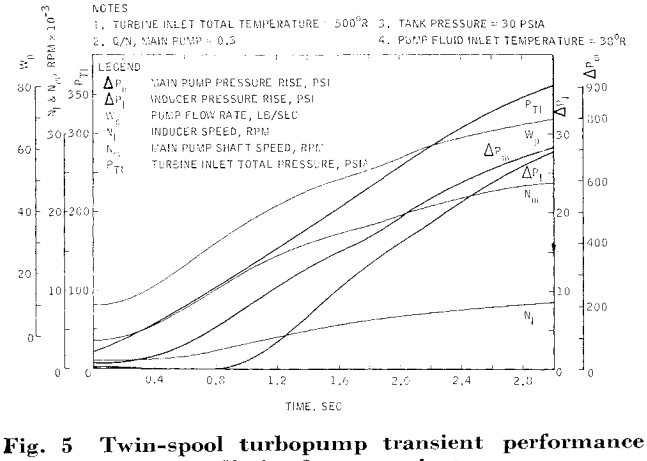

Fig. 5 Twin-spool turbopump transient performance prediction 3-sec transient.

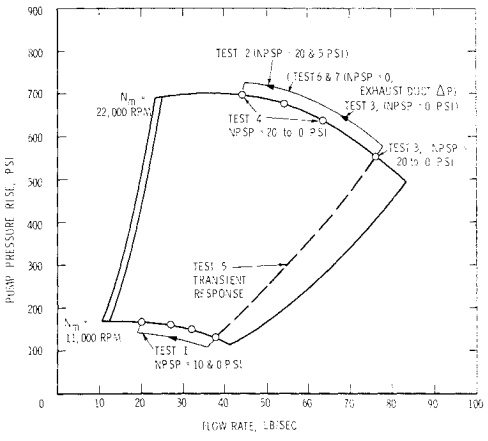

Fig. 6 Twin-spool turbopump test outline.

This indicated incipient vaporization of the fluid as it began to enter the liquid-vapor dome of the T-S diagram for hydrogen and ensured zero NPSP at the pump. Vaporization first begins at station 26 because of the reduction of static pressure as the flow is accelerated into the 10-in. line from the 24-in. section.

The amount of vapor ingested, by the inducer, is determined by using the fluid saturation temperature and the measured static pressure. The saturation temperature and the saturation line on the liquid vapor dome establish the entropy (S) of the propellant. Assuming that entropy is constant ($\Delta S = 0$), the liquid vapor dome of the T-S diagram is entered on the constant S line to the measured static pressure. (A constant entropy approach yields a slightly more conservative vapor estimate, as opposed to a constant enthalpy process as used by some investigators.) At this point, the vapor by volume is estimated from the thermodynamic properties of the propellant.

Platinum resistance probes (Rosemount RTT) were used for measuring propellant temperatures in the pump suction and discharge line. The estimated 2σ systems accuracy was 0.069°F, resulting in a possible vapor pressure error of 0.2 psi. The 1σ system accuracy was estimated at 0.3% of the full range value (0 to 60 psi). Flow-meter accuracy was estimated to be within 1% of the flow rates tested.

Test Results

The test matrix was completed in seven tests with all data achieved in one test less than planned. Full-speed operation

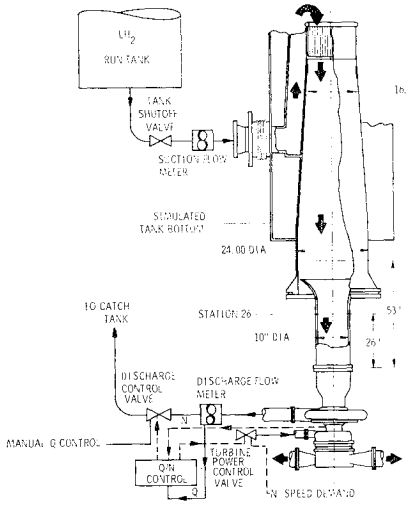

Fig. 7 Twin-spool turbopump test setup schematic.

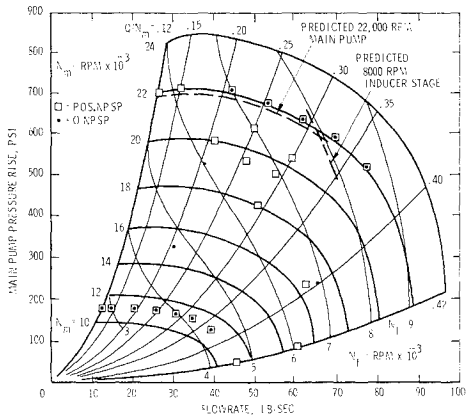

Fig. 8 Twin-spool operating map and test data.

occurred for a cumulative time of 45 min., with a total run time of 64 min.

Figure 8 shows the pump operating map. The inducer speed lines are shown as a function of the main turbopump speed and its related Q/N value. For comparison, the 22,000 rpm main turbopump speed line from the predicted map (Fig. 4) is superimposed upon the actual operating map. The main pump pressure rise at a constant speed line appears to be higher than the predicted curve. This may be due to a combination of prewhirl effect and the main pump i/β relationship. (Ratio of the fluid incidence angle to the blade angle, incidence being the blade angle less the fluid angle.) The inducer speed line is compared in a similar manner at 8000 rpm.

The data points in Fig. 8 are indicated as a function of their corresponding inlet NPSP. The inlet NPSP has no effect upon the main pump performance. The data points at Q/N values of 0.42, 0.15, and 0.123 (stall) were actually taken at NPSPs of 1.0, 1.0, and 1.5 psi, respectively. As evidenced by a comparison between Figs. 8 and 3, the addition of the low-speed inducer had a significant effect upon the operating characteristics of the main stage pump at very low and zero NPSP. Both pressure rise and flow range were significantly improved.

Figure 9 shows the over-all turbopump pressure rise vs flow rate for a main pump shaft speed of 22,000 rpm. The main pump pressure rise is shown in the lower curve with the sum of the inducer and main pump pressure rise being the upper curve. Inlet conditions at NPSP values of 15 and 0 psi (saturation) are presented. Although they are not shown, the efficiencies of the inducer and main pump were nominal. The inducer showed some efficiency loss, as would be expected, as the NPSP was lowered and vapor ingestion occurred.

The operating speed ratio (main turbopump speed divided by inducer stage speed) was within $\frac{1}{2}\%$ of that predicted at the $Q/N = 0.29$ point, and the actual speed-to-predicted-speed ratio error did not exceed 3% within the nominal operating range defined as $Q/N = 0.214$ to $Q/N = 0.364$. As Q/N approaches the stall limit for the main pump ($Q/N = 0.123$), the speed ratios are not as close because of the in-

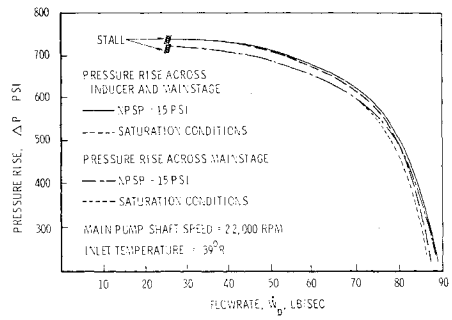

Fig. 9 Pressure rise vs flow rate.

accurate prediction at the wide flow excursion of the inducer from its nominal operating range.

Figure 10 shows representative plots of main and inducer stage head coefficients vs inlet NPSP or vapor ingestion V_g/V_m (fraction by volume) for main pump Q/N values of 0.214, 0.295, and 0.364, respectively. The inducer stage head coefficient drops only slightly as the inlet conditions approach zero NPSP, and the main pump shows no significant shift. As the inlet conditions enter the liquid-vapor dome of the T-S diagram, the inducer stage pressure rise begins to show some loss, but the main pump continues to operate in an essentially noncavitating condition even with $V_g/V_m = 0.1$.

At the Q/N value of 0.295 (see Fig. 10, center) data were acquired with V_g/V_m up to nearly 0.5. These data clearly indicate the ability of the inducer stage to provide the main pump inlet with sufficient NPSP while ingesting up to 30% vapor, over part of the operating range. The head loss on the main pump was 7% at an inducer V_g/V_m of 0.44; the inducer at this point incurred a pressure rise loss of 80%. It should be noted that temperature was 37.3°R at the point where the liquid hydrogen entered the liquid vapor dome.

Figure 11 shows significant turbopump parameters plotted in relationship to time. As the NPSP approaches zero and vapor formation begins, the shaft speeds shift slightly, but the normalized pressure rise and flow rates remain almost constant. No significant changes are seen until the vapor level has reached approximately 30% by volume.

Figure 12 shows a comparison of the twin-spool turbopump inducer performance with two NASA inducer configurations. Inducer cavitating loss at zero NPSP is plotted as a function of incidence-to-blade-angle ratio. (Incidence is defined as the tip blade angle less the fluid angle.)

Noncavitating main-stage performance was maintained at NPSPs of 1.5 psi or less for a flow range from $Q/N = 0.12$ to $Q/N = 0.42$. When comparing the data just discussed to the performance shown in Fig. 3, it is evident that the twin-spool turbopump concept offers the capability for significantly extending the useful operating range of turbopump at very low and zero values of NPSP.

The transient response capability of the twin-spool turbopump is shown graphically in Fig. 13. The NPSP was set so that it reached 1 psi at the end of the ramp (for this particular test). The inducer tracked well with the main turbopump, which would be expected due to the close coupling of

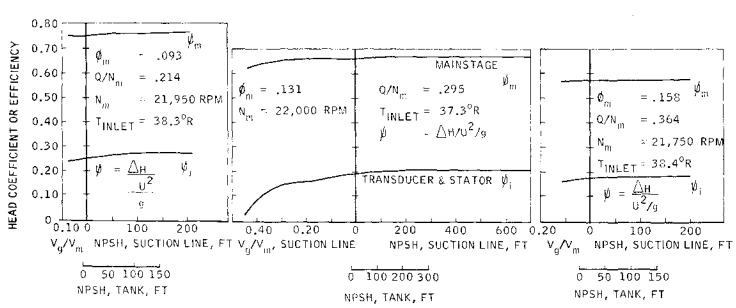

Fig. 10 Head coefficient and efficiency vs NPSH and vapor by volume.

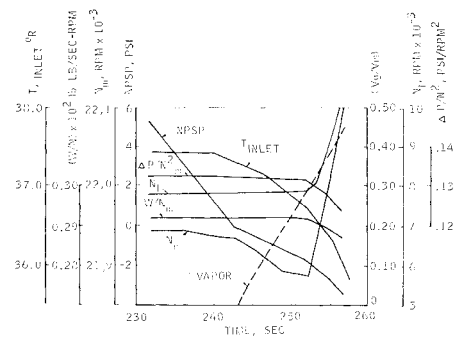

Fig. 11 Twin-spool turbopump data $Q/N = 0.295$ test 003.

the main and inducer turbines. Transient response while traversing from data point to data point was excellent, even when the turbine exhaust line was orificed and the available inducer turbine drive power was less than nominal. A similar start ramp was made with a 20-psi terminal NPSP setting. The plots are essentially identical. In addition, a 6-sec ramp was made with a terminal NPSP of 0 psi. Again, the speed ratios were similar, with the inducer responding well over the entire ramp.

Two tests were conducted to study the sensitivity of the inducer stage to variations in the turbine exhaust system. In these tests, the effective turbine exhaust area was reduced by 10% and 20%. Figure 14 shows the ratio of the main turbopump to inducer stage shaft speed for various values of main stage Q/N. The speed ratio profiles illustrates that tuning of an exhaust system is not a mandatory requirement when considering a twin-spool turbopump for a given engine application. The actual reduction of the inducer shaft speed from the nominal 8400 rpm was approximately 150 rpm and 500 rpm for the 10% and 20% reduction at $Q/N = 0.364$.

Conclusions

The following significant conclusions can be drawn from this series of tests. The twin-spool turbopump can operate without cavitation over a wide range of flow rates at zero NPSP while ingesting significant quantities of vapor at the pump inlet. Its transient response characteristics are excellent for either chemical or nuclear engine applications.

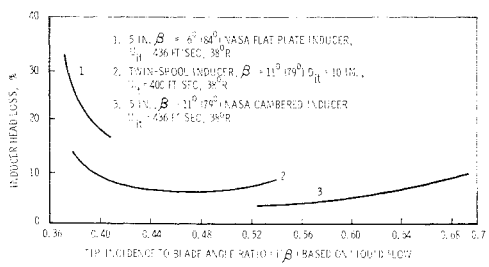

Fig. 12 Inducer head loss vs i/β ratio.

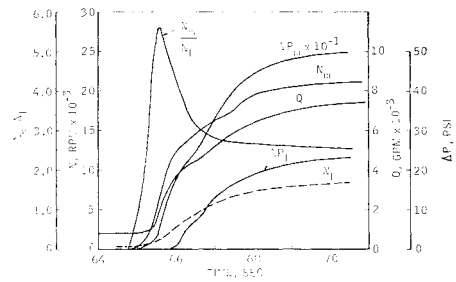

Fig. 13 Twin-spool turbopump start ramp at N_m (max) = 1 psi.

The inducer stage is relatively insensitive to reasonable variations in the turbine exhaust system pressure losses. Performance and operational behavior, both steady-state and transient, are as predictable as those of its individual component characteristics.

The stall margin of the pump is not reduced when operating at low and zero values of suction pressure. The twin-spool turbopump can make the engine system almost insensitive to variation in tank pressure (no amplification) and hydrodynamically decouples the tank from the engine, making engine thrust independent of tank conditions.

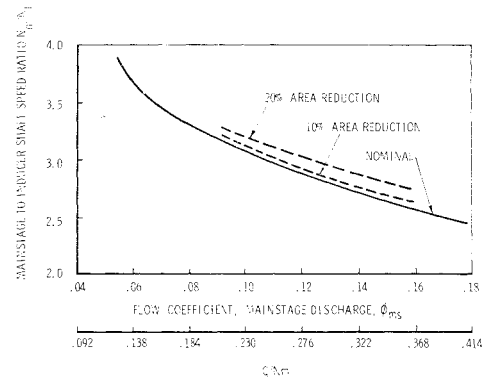

Fig. 14 Shaft speed ratio vs flow coefficient and Q/N.

References

[1] Campbell, W. F., "Zero NPSP Pumping Tests with an Operational Hydrogen Turbopump," *9th Liquid Propulsion Symposium*, Oct. 25–27, 1967, St. Louis, Mo.

[2] Campbell, W. E., Beveridge, J. H., and Fitts, J. J., "NPSP Selection for a Nuclear Rocket," AIAA Paper 67-476, Washington, D. C., 1967.

[3] Meng, P. R. and Connelly, R. E., "Investigation of Effects of Simulated Nuclear Radiation on Inducer Performance in Liquid Hydrogen," TM X-1359, NASA.

[4] DiStefano, J. F. and Caine, G. H., "Development of Tank-Mounted Hydrogen and Oxygen Booster Pumps for Space Vehicles," American Rocket Society, Space Flight Report to the Nation, New York Coliseum, Sept. 15, 1961.

[4] "Postflight Evaluation of Atlas-Centaur AC-8 NASA, Lewis Research Center," TM E-3563 (review copy), NASA.